Biochemical Pharmacology 77 (2009) 1337–1347

Contents lists available at ScienceDirect

Biochemical Pharmacology

journal homepage: www.elsevier.com/locate/biochempharm

A novel resveratrol derivative, HS1793, overcomes the resistance conferred by Bcl-2 in human leukemic U937 cells

Seung Hun Jeong [a], Wol Soon Jo [b], Suhee Song [c], Hongsuk Suh [c], So-Young Seol [d], Sun-Hee Leem [d], Taeg Kyu Kwon [e], Young Hyun Yoo [a,*]

[a] Department of Anatomy and Cell Biology, Dong-A University College of Medicine and Medical Science Research Center, 3-1 Dongdaesin-dong, Seo-gu, Busan 602-714, South Korea
[b] Department of Immunology, Dong-A University College of Medicine, Busan 602-714, South Korea
[c] Department of Chemistry and Chemistry Institute for Functional Materials, Pusan National University, Busan 609-735, South Korea
[d] Department of Biological Science, Dong-A University, Busan 604-714, South Korea
[e] Department of Immunology and Chronic Disease Research Center and Institute for Medical Science, School of Medicine, Keimyung University, 194 DongSan-Dong, Jung-Gu, Taegu 700-712, South Korea

ARTICLE INFO

Article history:
Received 6 December 2008
Accepted 2 January 2009

Keywords:
Bcl-2
14-3-3
Resveratrol
Leukemia
Apoptosis

ABSTRACT

The chemopreventive and chemotherapeutic properties associated with resveratrol offer promise for the design of new chemotherapeutic agents. However, resveratrol is not a potent cytotoxic compound when compared with other chemotherapeutic drugs. Thus, several studies were undertaken to obtain synthetic analogues of resveratrol with potent activity. The present study was undertaken to examine whether four resveratrol analogues (HS-1784, -1792, -1791 and -1793) that we had designed and synthesized show antitumor activity. Here, we observed that all of these resveratrol analogues displayed stronger antitumor effects than resveratrol in most cancer cells tested. We further examined whether HS-1793, showing potent antitumor effects in most cancer cells tested, overcomes the resistance conferred by Bcl-2, since overcoming the resistance conferred by Bcl-2 represents an attractive therapeutic strategy against cancer. Our viability assay showed that HS-1793 overcomes the resistance conferred by Bcl-2 in human leukemic U937 cells. Various apoptosis assessment assays demonstrated that HS-1793 overcomes the resistance conferred by Bcl-2 in human leukemic U937 cells by inducing apoptosis. Noticeably, we elucidated the marked downregulation of 14-3-3 protein by HS-1793, indicating that HS-1793 overcomes the resistance conferred by Bcl-2 in U937 cells via 14-3-3. We also observed that HS-1793 exerts its antitumor activity via Bad. However, overall data obtained from methylation specific PCR, RT-PCR and real-time PCR suggest that HS-1793 plays a role in the downregulation of 14-3-3 at a post-transcriptional level. Further understanding exactly how HS-1793 overcomes the resistance conferred by Bcl-2 via 14-3-3 may guide the development of future anticancer agents.

1. Introduction

Bcl-2 functions as an anti-apoptotic protein [1]. Bcl-2, in general, regulates mitochondrial outer membrane permeabilization and thereby determines the cellular commitment to apoptosis [1–3]. The anti-apoptotic function of the Bcl-2 protein depends, at least in part, on its ability to dimerize with another member of the Bcl-2 family, Bax [4]. Overexpression of Bcl-2 has been reported in a wide variety of cancers.

In some preclinical systems, Bcl-2 overexpression has been shown to attenuate apoptosis, or to restore the clonogenic potential of malignant progenitor cells [5,6]. On the other hand, anti-apoptotic factors, including Bcl-2, impair the ability to achieve remission and cure with chemotherapy, protecting the tumor cells from the apoptotic effects of various anti-neoplastic agents [7–9]. Therefore, overcoming the resistance conferred by anti-apoptotic factors such as Bcl-2 represents an attractive therapeutic strategy against leukemia cells [3]. We previously demonstrated that overexpression of Bcl-2 attenuates resveratrol-induced apoptosis in U937 cells by inhibition of caspase-3 activity and sustained expression of the IAP caspase inhibitors [6].

Resveratrol, a naturally occurring phytoalexin (3,4′,5-tri-hydroxystilbene) present in medicinal plants, grape skin, peanuts and red wine [10,11], acts on the process of carcinogenesis by affecting the three phases (tumor initiation, promotion and progression) and is also able to activate apoptosis [6,12–14]. The chemopreventive and chemotherapeutic properties associated with resveratrol offer promise for the design of new chemotherapeutic agents. However,

* Corresponding author. Tel.: +82 51 240 2926; fax: +82 51 241 3767.
E-mail address: yhyoo@dau.ac.kr (Y.H. Yoo).

0006-2952/$ – see front matter. Crown Copyright © 2009 Published by Elsevier Inc. All rights reserved.
doi:10.1016/j.bcp.2009.01.002

resveratrol is not a potent cytotoxic compound when compared with other chemotherapeutic drugs. Thus, exposure to high doses of resveratrol is required to induce apoptosis in cancer cells, including U937 cells [6,15–18]. Moreover, resveratrol's biological activity is limited by its photosensitivity and metabolic instability. Thus, several studies were undertaken to obtain synthetic analogues of resveratrol with potent activity.

The present study was undertaken to examine whether four resveratrol analogues that we had designed and synthesized [19] show antitumor activity. Here, we demonstrate that resveratrol analogues show stronger antitumor activity than resveratrol in various cancer cells. To further examine the mechanism underlying the antitumor activity, we employed a resveratrol derivative, 4-(6-hydroxy-2-naphthyl)-1,3-benzenediol (HS-1793), and human leukemic U937 cells. As will be shown, HS-1793 induces apoptosis and overcomes the resistance conferred by Bcl-2 in U937 cells through 14-3-3.

2. Materials and methods

2.1. Reagents

Rabbit polyclonal anti-human Bcl-2, cytochrome *C*, 14-3-3β, 14-3-3θ, glyceraldehyde-3-phosphate dehydrogenase (GAPDH) and mouse monoclonal anti-human 14-3-3 antibodies were obtained from Santa Cruz Biotechnology (Santa Cruz, CA). Mouse polyclonal anti-human Poly(ADP)-Ribose Polymerase (PARP) was obtained from Oncogene (Cambridge, MA). Rabbit polyclonal anti-human caspase-3 and -6 antibodies were obtained from Cell Signaling Technology (Danvers, MA). Fluorescein isothiocyanate (FITC)-conjugated goat anti-rabbit and horse anti-mouse IgG antibodies were obtained from Vector (Burlingame, CA). HRP-conjugated donkey anti-rabbit and sheep anti-mouse IgG antibodies were obtained from Amersham Pharmacia Biotech (Piscataway, NJ). JC-1 was obtained from Molecular Probes (Eugene, OR). Neomycine sulfate (G418) was from Calbiochem (Canada, U.S.). DMEM, MEM, RPMI-1640 and fetal bovine serum (FBS) were obtained from Gibco (Gaithersburg, MD). The enhanced chemiluminescent western blotting detection reagent (SuperSignal West Pico chemiluminescent substrate) was obtained from Pierce (Rockford, IL). Resveratrol and propidium iodide were obtained from Sigma (St. Louis, MO).

2.2. Preparation of resveratrol analogues

To obtain analogues with improved antitumor activity, we substituted the stilbene double bond present in resveratrol with a naphthalene ring.

2.2.1. General procedure of coupling

2-Bromo-6-methoxy-naphthalene, 5-bromo-1,2,3-trimethoxy-benzene, 1-bromo-3-methoxy-benzene, and 1-bromo-2,4-dimethoxy-benzene were slowly added to the mixture of magnesium turnings (1 equiv.) and iodine (cat.) in THF. After the formation of the Grignard reagent (2 h, reflux), a solution of 1-bromo-3,5-dimethoxy-benzene (0.5 equiv.) in THF was slowly added to the Grignard reagent. The reaction mixture was stirred overnight under reflux, cooled to room temperature, poured onto ice containing HCl solution, extracted with ether, dried over $MgSO_4$. The combined organic extract was concentrated under reduced pressure, and the solid residue was purified by flash chromatography to give brown solid of 2-phenyl-naphthalene.

2.2.2. 2-(3,5-Dimethoxyphenyl)-6-methoxy-naphthalene

mp 77 °C; ^{1}H NMR (300 MHz, Benzene-D_6) δ 3.39 (s, 6H), 3.40 (s, 3H), 6.64 (t, 1H, J = 2.5 Hz), 6.96 (d, 1H, J = 2.5 Hz), 7.03 (d, 2H, J = 1.8 Hz), 7.21 (dd, 1H, J = 8.3 and 2.4 Hz), 7.55 (d, 1H, J = 9.1 Hz), 7.65 (d, 1H, J = 8.5 Hz), 7.75 (dd, 1H, J = 8.5 and 1.9 Hz), 7.99 (s, 1 Hz); ^{13}C NMR (75 MHz, Benzene-D_6) δ 55.13, 55.27, 100.26, 106.20, 106.37, 119.98, 126.62, 126.84, 127.96, 130.06, 130.51, 134.93, 137.41, 144.32, 158.67, 162.23; HRMS (EI), m/z 294.1257 (calculated for $C_{19}H_{18}O_3$ 294.1256).

2.2.3. 2-Methoxy-6-(3,4,5-trimethoxyphenyl)-naphthalene

mp 74 °C; ^{1}H NMR (300 MHz, Benzene-D_6) δ 3.43 (s, 3H), 3.46 (s, 6H), 3.94 (s, 3H), 6.89 (s, 2H), 7.02 (d, 1H, J = 2.5 Hz), 7.25 (dd, 1H, J = 8.8 and 2.5 Hz), 7.63 (d, 1H, J = 9.1 Hz), 7.75 (s, 1H), 7.76 (d, 1H, J = 1.7 Hz), 8.01 (s, 1H); ^{13}C NMR (75 MHz, Benzene-D_6) δ 54.74, 55.78, 60.49, 105.42, 105.88, 119.58, 125.82, 126.39, 127.49, 127.88, 129.65, 129.88, 134.26, 137.17, 137.25, 154.34, 158.18; HRMS (EI), m/z 324.1359 (calculated for $C_{20}H_{20}O_4$ 324.1362).

2.2.4. 2-Methoxy-6-(3-methoxyphenyl)-naphthalene

mp 84 °C; ^{1}H NMR (300 MHz, Benzene-D_6) δ 3.38 (s, 3H), 3.39 (s, 3H), 6.83 (d, 1H, J = 7.6 Hz), 6.95 (s, 1H), 7.16–7.30 (m, 3H), 7.35 (s, 1H), 7.54 (d, 1H, J = 9.1 Hz), 7.65 (d, 1H, J = 8.5 Hz), 7.71 (d, 1H, J = 8.6 Hz), 7.94 (s, 1H); ^{13}C NMR (75 MHz, Benzene-D_6) δ 55.13, 106.24, 113.33, 113.80, 119.99, 120.53, 126.65, 126.83, 130.15, 130.50, 130.53, 134.88, 137.25, 143.66, 158.70, 161.11; HRMS (EI), m/z 264.1149 (calculated for $C_{18}H_{16}O_2$ 264.1150).

2.2.5. 2-(2,4-Dimethoxyphenyl)-6-methoxy-naphthalene

mp 99 °C; ^{1}H NMR (300 MHz, Benzene-D_6) δ 3.25 (s, 3H), 3.39 (s, 3H), 3.41 (s, 3H), 6.48 (d, 1H, J = 9.2 Hz), 6.58 (s, 1H), 6.99 (s, 1H), 7.21 (d, 1H, J = 8.8 Hz), 7.38 (d, 1H, J = 8.5 Hz), 7.59 (d, 1H, J = 9.0 Hz), 7.72 (d, 1H, J = 8.6 Hz), 7.88 (d, 1H, J = 8.5 Hz), 8.00 (s, 1H); ^{13}C NMR (75 MHz, Benzene-D_6) δ 55.12, 55.33, 55.43, 100.04, 105.39, 106.26, 119.49, 124.67, 12.79, 128.73, 129.71, 130.04, 130.33, 132.27, 134.34, 135.03, 158.43, 158.62, 161.26; HRMS (EI), m/z 294.1255 (calculated for $C_{19}H_{18}O_3$ 294.1256).

2.2.6. General procedure of demethylation

To a stirred solution of prepared product in CH_2Cl_2 at −78 °C was added BBr_3 (5 equiv.). The resulting yellow solution was stirred at −78 °C for 20 min and then was allowed to warm to room temperature and stirred for 6 h. The mixture was then washed with water to neutrality. The organic layer was separated and dried over $MgSO_4$. The combined organic extract was concentrated under reduced pressure, and the solid residue was purified by flash chromatography to give brown solid of naphthol.

2.2.7. 5-(6-Hydroxy-2-naphthyl)-1,3-benzenediol

mp 189 °C; ^{1}H NMR (300 MHz, Benzene-D_6) δ 6.85 (t, 1H, J = 2.2 Hz), 7.12 (d, 2H, J = 2.2 Hz), 7.30 (dd, 1H, J = 2.5, 8.8 Hz), 7.40 (d, 1H, J = 2.5 Hz), 7.60 (s, 1H), 7.63 (s, 1H),7.74 (dd, 1H, J = 1.6, 8.5 Hz), 8.04 (d, 1H, J = 1.4 Hz); ^{13}C NMR (75 MHz, Benzene-D_6) δ 102.0, 106.6, 109.8, 119.1, 126.0, 126.3, 127.0, 129.3, 130.8, 135.0, 138.5, 144.8, 155.9, 159.9; HRMS (EI), m/z 252.0785 (calculated for $C_{16}H_{12}O_3$ 252.0786).

2.2.8. 5-(6-Hydroxy-2-naphthyl)-1,2,3-benzenetriol

mp 215 °C; ^{1}H NMR (Benzene-D_6) δ (ppm): 7.13 (s, 2H), 7.28 (dd, 1H, J = 2.5, 8.8 Hz), 7.37 (d, 1H, J = 2.5 Hz), 7.62 (dd, 1H, J = 1.9, 8.8 Hz), 7.71 (dd, 1H, J = 1.9, 8.5 Hz), 7.98 (d, 1H, J = 1.6 Hz); ^{13}C NMR (75 MHz, Benzene-D_6) δ 107.4, 109.8, 119.8, 125.7, 126.6, 127.8, 129.8, 130.5, 133.4, 134.2, 134.9, 136.9, 147.0, 155.8; HRMS (EI), m/z 268.0733 (calculated for $C_{16}H_{12}O_4$ 268.0736).

2.2.9. 6-(3-Hydroxyphenyl)-2-naphthol

mp 174 °C; ^{1}H NMR (300 MHz, Benzene-D_6) δ 7.08 (dt, 1H, J = 1.9, 7.1 Hz), 7.26 (t, 1H, J = 8.4 Hz), 7.33 (dd, 1H, J = 2.5, 8.8 Hz), 7.41 (d, 1H, J = 2.5 Hz), 7.50 (d, 1H, J = 1.6 Hz), 7.65 (d, 2H,

J = 8.8 Hz), 7.68 (dd, 1H, J = 1.6, 8.2 Hz), 7.98 (s, 1H); ^{13}C NMR (75 MHz, Benzene-D_6) δ 109.8, 114.8, 115.0, 119.5, 126.4, 126.6, 127.5, 129.7, 130.6, 130.7, 135.3, 136.7, 143.8, 156.2, 158.5; HRMS (EI), m/z 236.0834 (calculated for $C_{16}H_{12}O_2$ 236.0837).

2.2.10. 4-(6-Hydroxy-2-naphthyl)-1,3-benzenediol

mp 186 °C; ^{1}H NMR (300 MHz, Benzene-D_6) δ 6.72 (dd, 1H, J = 2.2, 8.5 Hz), 6.86 (d, 1H, J = 2.5 Hz), 7.23 (dd, 1H, J = 2.5, 8.8 Hz), 7.28 (d, 1H, J = 8.5 Hz), 7.37 (d, 1H, J = 2.5 Hz), 7.60 (d, 1H, J = 5.8 Hz), 7.62 (d, 1H, J = 5.5 Hz), 7.78 (dd, 1H, J = 1.6, 8.5 Hz), 7.98 (s, 1H); ^{13}C NMR (75 MHz, Benzene-D_6) δ 104.0, 108.4, 109.8, 119.1, 121.9, 126.7, 127.4, 129.3, 129.7, 130.4, 132.5, 134.6, 134.7, 155.8, 156.1, 158.5; HRMS (EI), m/z 252.0790 (calculated for $C_{16}H_{12}O_3$ 252.0786).

2.3. Cell culture and establishment of Bcl-2-overexpressing U937 cells

Human leukemia U937 cells were obtained from the American Type Culture Collection (ATCC; Rockville, MD). The culture medium used throughout these experiments was RPMI-1640 medium, containing 10% fetal calf serum (FCS), 20 mM HEPES buffer and 100 μg/ml gentamicin. Bcl-2-overexpressing U937 cells were generated using a pMAX vector containing the human *bcl-2* gene (provided by Dr. Rakesh Srivastava, NIH/NIA). U937 cells (400 μl) in RPMI 1640 (20×10^6 cells/ml) were transfected by pre-incubating with 15 μg Bcl-2 plasmid for 10 min at room temperature and then electroporating at 500 V, 700 μF. The sample was immediately placed on ice for 10 min, then 10 ml of complete medium was added, and the cells were incubated at 37 °C for 24 h. The cells were selected in a medium containing 0.7 μg/ml geneticin (G418) for 4 weeks. Single cell clones were obtained by limiting dilution and subsequently analyzed for an increase in Bcl-2 protein expression relative to identically cloned empty vector controls.

2.4. Resveratrol and resveratrol analogues treatment and assessment of cell viability

Ten millimolars of resveratrol analogues and 100 mM of resveratrol in EtOH were prepared and stored at −80 °C until use. Cells were treated with resveratrol analogues (0–5 μM) or resveratrol (0–120 μM). Cells were harvested 48 h after treatment, and cell viability was determined with the Vi-Cell cell counter (Beckman Counter, Fullerton, CA), which performs an automated trypan blue exclusion assay.

2.5. Clonogenic study

The clonogenic assay was performed on a single-cell suspension of exponentially growing cells. Stock agar solution was prepared by dissolving agar (Sigma; St. Louis, MO) in bidistilled water and autoclaving at 120 °C under 1 atm of pressure and kept at 45 °C until use. Four volumes of RPMI-1640 were then rapidly mixed with one volume of stock agar solution, and 1 ml of this solution was placed into each well of a 6-well plate as an underlayer. Plates were then incubated at 4 °C for 15 min. For each well, 200 100% vital cells were suspended in 1 ml of RPMI-1640 medium. They were then mixed with 2 ml of the mixture of 4 volumes of RPMI-1640 plus 1 volume of stock agar solution. One millilitre of this suspension was then put into each underlayer of the 6-well plate, and drugs were added to a final volume of 100 μl to the corresponding group. The 6-well plates were then kept in an incubator in a humidified atmosphere of 5% CO_2 and air-mixed for 14 days. Colonies with more than 50 cells were counted under an inverted microscope. Calculation of survival fraction (SF) was performed using the equation SF = colonies counted/cells seeded × (PE/100), taking the individual plating efficiency (PE) into consideration.

2.6. Nuclear morphology analysis of apoptosis

Twenty-four hours after treatment, the cell suspension was cytospun onto a clean fat-free glass slide with a cytocentrifuge. Cytocentrifuged samples were fixed for 10 min in 4% paraformaldehyde and stained in 4 μg/ml Hoechst 33342 for 30 min at 4 °C. The total cell number (300 cells from each experiment) was counted using differential interference contrast (DIC) optics, and the number of cells showing condensed or fragmented nuclei on Hoechst staining was calculated using epifluorescence optics by an observer who was blinded with regard to the experimental group.

2.7. Methylation-specific polymerase chain reaction (MSP)

Genomic DNA was extracted using the Qiagen QIAamp DNA Mini Kit (Qiagen, Hilden, Germany). Bisulphite treatment of 2 μg DNA of each sample was undertaken using the EZ DNA Methylation Kit™ (ZYMO Research Co., Orange, CA). Two primer sets were used for MSP amplification of 14-3-3β as follows: methylated 1 (14-3-3β-M1, F-AGAGGATTGATATCGGTTTTC & R-ACTAAAAACGCGCCAAAA) and unmethylated 1 (14-3-3β-UnM1, F-GTAAGAGGATTGATATTG-GTTTTT & R-ACTAAAAACACACCAAAACCA); methylated 2 (14-3-3β-M2, F-GGAGCGGAAGTGGAGTTATC & R-CCCACTACTCAAACGAC-GAC) and unmethylated 2 (14-3-3β-UnM2, F-GGAGTGGAAGTG-GAGTTATT & R-CCCACTACTCAAACAACAAC). All PCR primers used in this work were designed using Methyl Primer Express® Software (www.appliedbiosystems.com/methylprimerexpress), based on the NCBI site (>ref|NC_000020.9|NC_000020:42945759-42970575 Homo sapiens chromosome 20, reference assembly, complete sequence, homo sapiens build 36.3). MSP PCR reactions (50 μl) were performed in reaction mixes containing 2 μl of bisulfate-treated DNA, 10 μM primers, 100 ng/μl TITANIUM™ Taq DNA polymerase (Takara, Japan), 1× TITANIUM™ *Taq* PCR Buffer and 0.2 mM dNTPs. PCR was performed in a 9700 Thermocycler (PerkinElmer, CT, USA), and the general thermocycling conditions were as follows: (1) one cycle of 5 min of initial denaturation at 95 °C, followed by 35 cycles of 30 s at 95 °C, annealing for 30 s at 56 °C and reaction for 45 s at 72 °C, and then a final 10 min extension at 72 °C for 14-3-3β-M1 and 14-3-3β-UnM1; (2) one cycle of 5 min of initial denaturation at 95 °C, followed by 35 cycles of 30 s at 95 °C, annealing for 30 s at 59 °C and reaction for 45 s at 72 °C, and then a final 10 min extension at 72 °C for 14-3-3β-M2 and 14-3-3β-UnM2. PCR products were separated by gel electrophoresis using 3% SeaKem LE agarose (Cambrex, ME, USA) in 1× TAE buffer.

2.8. Quantitative reverse transcriptase (RT)-PCR

For RT-PCR of 14-3-3β and 14-3-3θ mRNA, total RNA was extracted from U937/vector and U937/Bcl-2 cells using the RNeasy plus Mini kit (QIAGEN) following the manufacturer's instructions. RT reactions were performed with the iScript™ cDNA Synthesis Kit for RT-PCR (Bio-Rad) using 1 μg of fractionated cellular RNA, which was purified as described above, as a template. Real-time PCR was carried out using TaqMan gene expression pre-synthesized reagents and iTaq™ Super mix with ROX (Bio-Rad). Reactions were prepared following the manufacturer's protocol. All reactions were carried out in triplicate (Bio-Rad). Specific primers were used to detect the presence of the 14-3-3β and 14-3-3θ mRNAs. Standard thermal cycling conditions included a hot start of 2 min at 50 °C and 10 min at 95 °C. The DNA was amplified through 50 cycles of 15 s at 95 °C and 1 min at 60 °C for STAT3 and β-actin, respectively. Data analysis was carried out using MJ Opticon Monotor 3 software (version 3.1) and Microsoft Excel.

Expression values are presented relative to the measurements for β-actin values in the corresponding samples.

2.9. RT-PCR

Total RNA was extracted from the cultured cells using the Qiagen RNaesy Mini Kit. Total RNA (2 μg) was converted to cDNA using a Thermoscript reverse transcriptase kit (Invitrogene, Carlsbad, CA, USA) according to the manufacturer's instructions.

RT-PCR products containing 14-3-3β exon 2 were amplified using gene a specific primer (F-GCTGAGCAGGCTGAGCGATA & R-TTGCCCATCTGCTGCTTCTTC). PCR reactions (40 μl) were performed in reaction mixes containing 3 μl cDNA, 10 μM primers, 2.5 U Go Taq Flexi DNA polymerase (Promega, WI, USA), 50 mM KCl, 10 mM Tris–HCl (pH 9.0), 3.0 mM $MgCl_2$ and 0.2 mM dNTPs. PCR was performed in a 9700 Thermocycler (PerkinElmer, CT, USA), and the general thermocycling conditions were as follows: one cycle of 2 min of initial denaturation at 94 °C, followed by 25 cycles of 30 s at 94 °C, annealing for 20 s at 64 °C and reaction for 30 s at 72 °C, followed by a final 7 min extension at 72 °C. PCR products were separated by gel electrophoresis using 2% SeaKem LE agarose in 1× TAE buffer.

2.10. DNA electrophoresis

Cells (2×10^6) were resuspended in 1.5 ml lysis buffer (10 mM Tris [pH 7.5], 10 mM EDTA [pH 8.0], 10 mM NaCl and 0.5% sodium dodecyl sulfate [SDS]), to which proteinase K (200 μg/ml) was added. After samples were incubated overnight at 48 °C, 200 μl of ice-cold 5 M NaCl was added and the supernatant containing fragmented DNA was collected after centrifugation. The DNA was then precipitated overnight at −20 °C in 50% isopropanol and treated with RNase A for 1 h at 37 °C. A loading buffer containing 100 mM EDTA, 0.5% SDS, 40% sucrose and 0.05% bromphenol blue was added to the DNA samples at a ration of 1:5 (v/v). Separation was performed in 2% agarose gels in Tris/acetic acid/EDTA buffer containing 0.5 μg/ml ethidium bromide (EtBr) at 50 mA for 1.5 h.

2.11. Flow cytometric analysis

Ice-cold 95% ethanol supplemented with 0.5% Tween 20 was added to cell suspensions to a final concentration of 70% ethanol. Fixed cells were pelleted and washed in 1% BSA-PBS solution. Cells were re-suspended in 1 ml PBS containing 11 Kunitz U/ml RNase, incubated at 4 °C for 30 min, washed once with BSA-PBS, and re-suspended in a PI solution (50 μg/ml). The cells were incubated at 4 °C for 30 min in the dark and were then washed with PBS. DNA content was measured on an Epics XL (Beckman Coulter, FL, USA), and the data were analyzed using Multicycle software, which allowed for simultaneous estimation of cell cycle parameters and apoptosis.

2.12. Western blot analysis

Conducted as described previously [20,21]. In brief, cell lysates were centrifuged at 14,000 rpm for 15 min at 4 °C. Protein concentrations of cell lysates were determined with Bradford protein assay (Bio-Rad) and 50 μg of proteins was loaded onto 7.5–15% SDS-polyacrylamide gels. The gels were transferred to Nitrocellulose membrane (Amersham Pharmacia Biotech, Piscataway, NJ) and reacted with each antibody. Immunostaining with antibodies was performed using Super-Signal West Pico enhanced chemiluminescence substrate and detected with LAS-3000PLUS (Fuji Photo Film Company, Kanagawa, Japan).

2.13. Assay of mitochondrial membrane potential (MMP)

3,3′ dihexyloxa carbocyanine iodide ($DIOC_6$) was added directly to the cell culture medium (1 μM final concentration). After a 30-min incubation, the cells were pelleted and resuspended with PBS. The cells were submitted to flow cytometry on the Epics XL (Beckman Coulter) to measure the MMP. Data were acquired and analyzed using EXPO32 ADC XL 4 color software. The analyzer threshold was adjusted on the forward scatter channel to exclude noise and most of the subcellular debris.

2.14. Immunofluorescent staining and confocal microscopy

Cytocentrifuged cells were fixed for 10 min in 4% paraformaldehyde, incubated with each primary antibody for 1 h, washed 3× for 5 min each and then incubated with FITC-conjugated secondary antibodies for 1 h at room temperature. Fluorescent images were observed and analyzed under a Zeiss LSM 510 laser-scanning confocal microscope (Zeiss, Gőettingen, Germany).

2.15. Coimmunoprecipitation assay

Conducted as described previously [20,21]. In brief, cells were collected and lysed in 1 ml of immunoprecipitation lysis buffer (300 mM NaCl, 50 mM Tris–Cl [pH 7.6], 0.5% Triton X-100, protease inhibitors, 10 mM $Na_4P_2O_7$, 1 mM Na_3VO_4, 25 mM NaF and 1 mM ß-glycerophosphate). Protein concentrations of cell lysates were determined using the Bradford method and 500 μg of protein was precleared and then incubated with PML or p53 antibody in extraction buffer at 4 °C overnight. The immune complexes were precipitated with protein A/G-agarose beads (Sigma) for 2 h and washed 5 times with extraction buffer prior to boiling in SDS sample buffer. Immunoprecipitated proteins were separated by SDS-polyacrylamide gel electrophoresis and Western blot analysis was performed as described above.

2.16. Statistical analysis

Four independent *in vitro* experiments were carried out. Statistical results were expressed as the mean ± standard deviation of the means obtained from triplicates of each independent experiment. Statistical significance of differences was determined by the paired Kruskal–Wallis nonparametric test. A *P*-value less than 0.05 was considered significant.

3. Results

3.1. Resveratrol analogues display antitumor activity in most cancer cell lines tested

The structures of four resveratrol analogues that we synthesized are shown in Fig. 1A. Depending on ^1H NMR, the purity of each compound was higher than 99%. We examined the antitumor activity of these 4 analogues using the following 9 different cancer cell lines: human breast adenocarcinoma cell line MCF-7; human hepatocellular carcinoma cell line HepG2; human colorectal adenocarcinoma cell line HT-29; human anaplastic thyroid cancer cell line KAT-18; human histiocytic lymphoma cell line U937; human chronic myelogenous leukemia cell line K562; human adenocarcinoma cell line HeLa; human carcinoma cell line LNCap; and human malignant melanoma cell line SK-MEL-28. Our data show that most resveratrol analogues displayed antitumor activity in all cancer cell lines tested. Most analogues in general had stronger antitumor effects than resveratrol in most of the cancer cells tested (Fig. 1B). Among these four analogues, HS-1784 and -1792 had the same structures as the analogues that have been

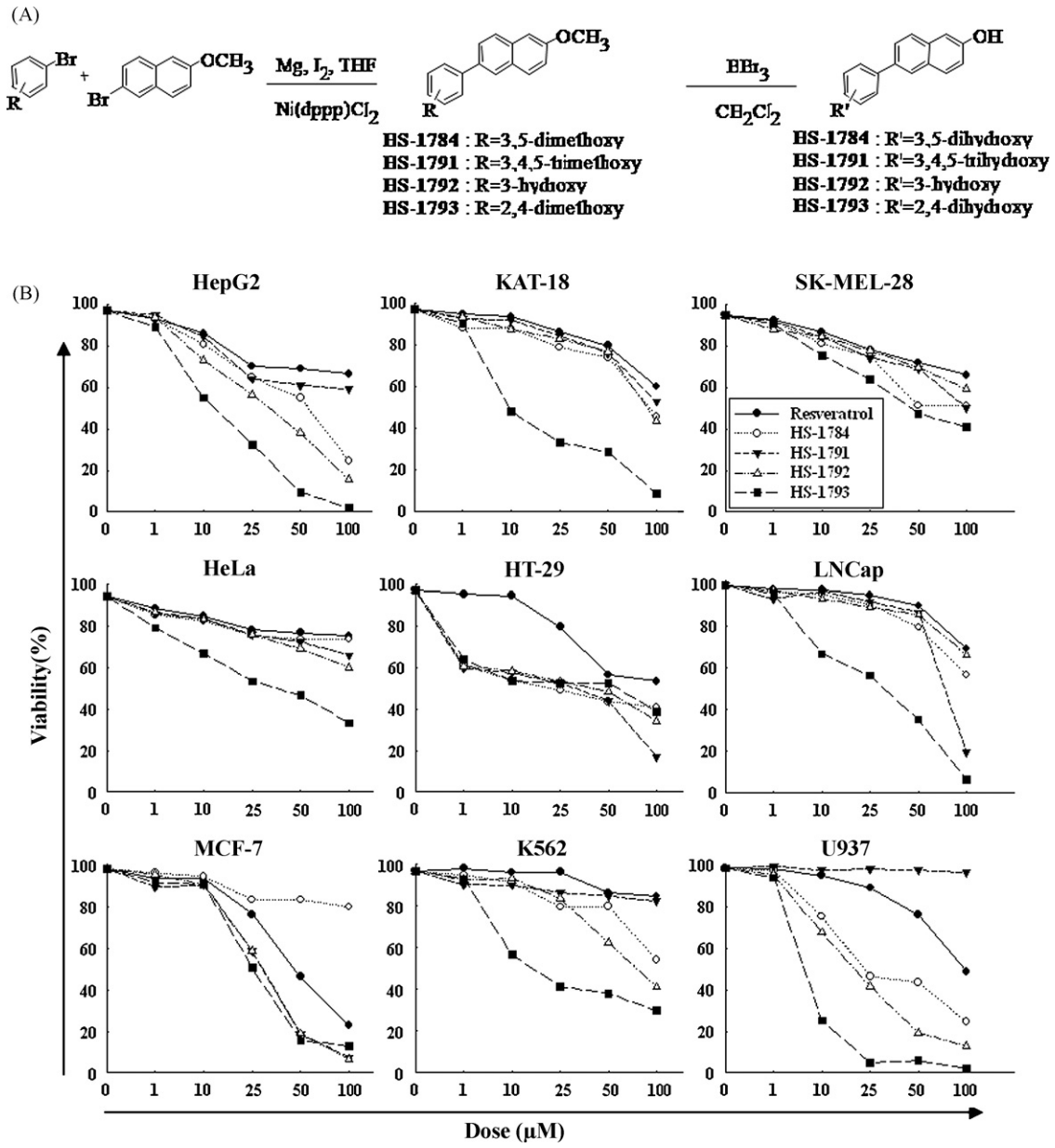

Fig. 1. Antitumor activity of synthetic resveratrol analogues. Synthesis of resveratrol analogues and their structures (Panel A). Resveratrol analogues show antitumor activity. Forty-eight hours after treatment, cell viability was determined with the Vi-cell counter performing an automated trypan blue exclusion assay (Panel B).

already reported [22–24]. In addition, a synthetic analogue having the same structure as HS-1784 was documented to have high ceramide-mediated proapoptotic activity in human breast cancer cells and to block the cell cycle in the G_0-G_1 phase in leukemia cells [22]. On the contrary, the synthesis of HS-1791 and -1793 has not been reported to date.

3.2. HS-1793 overcomes the resistance conferred by Bcl-2 in human leukemic U937 cells

HS-1793 showed relatively potent antitumor effects in most cancer cells tested. IC50 for MCF-7, HepG2, HT-29, KAT-18, U937, K562, HeLa, LNCap, and SK-MEL-28 cells is approximately 25, 15, 25, 10, 4, 20, 25, 30 and 50, respectively. Since overexpression of Bcl-2 attenuates resveratrol-induced apoptosis in U937 cells [6], we employed this novel single analogue to further examine whether HS-1793 overcomes the resistance by Bcl-2 in human leukemic cells. We first conducted a cell viability assay. Our viability assay demonstrated that HS-1793 overcomes the resistance by Bcl-2 in human leukemic cells. Although resveratrol at 20–120 μM significantly reduced the viability of U937/vector cells compared to the controls (control U937 and U937/vector cells), the overexpression of Bcl-2 significantly attenuated the resveratrol-induced reduction of viability. On the contrary, HS-1793 at 2–5 μM reduced the viability to a similar extent in both the U937/vector and U937/Bcl-2 cells (Fig. 2A). Long-term survival as determined by a clonogenic assay revealed a significant decline in clonogenic survival after treatment with HS-1793 ($\geq$1.5 μM) in U937, U937/vector and U937/Bcl-2 cells (Fig. 2B). These data suggest that HS-1793 overcomes the resistance conferred by Bcl-2 in human leukemic U937 cells. To examine whether or not HS-1793 counter Bcl-2 besides U937 cells, we conducted the viability assay on another cell line on which overexpression of Bcl-2 attenuates resveratrol-induced apoptosis. Our viability assay on

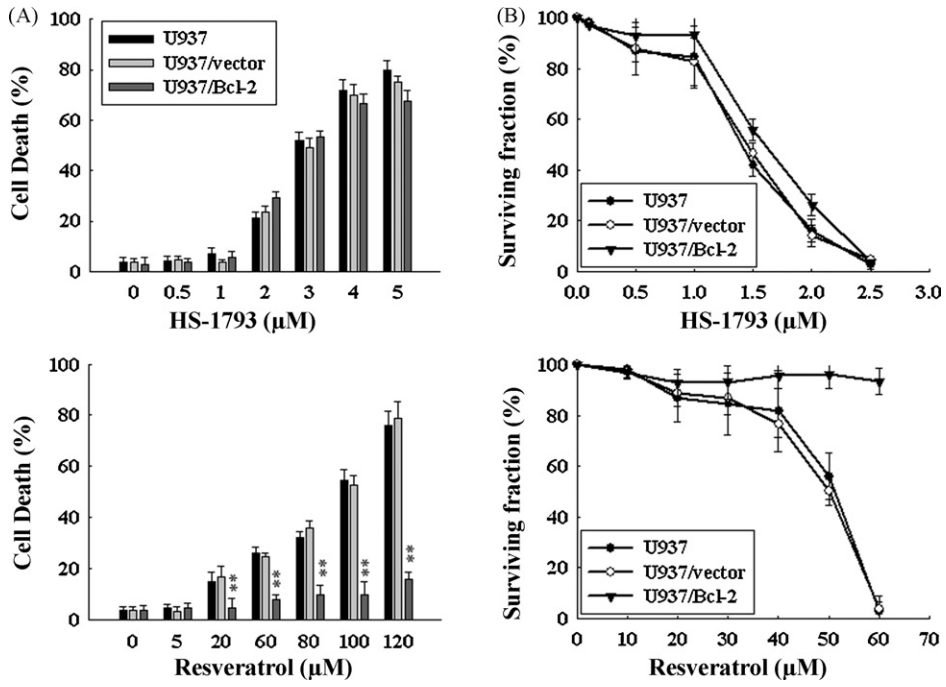

Fig. 2. HS-1793 overcomes the resistance conferred by Bcl-2 in U937 cells. Cell viability assay 48 h after treatment with resveratrol or HS-1793 shows that the overexpression of Bcl-2 significantly attenuated the resveratrol-induced reduction of viability whereas HS-1793 reduced the viability to a similar extent in both the U937/vector and U937/Bcl-2 cells. $^{**}P < 0.01$ comparing to controls (U937 control and U937/vector cells) (Panel A). Determination of cellular survival with clonogenic assay. Survival curves as determined by the clonogenic survival assay 14 days after HS-1793 or resveratrol treatment (Panel B).

human renal carcinoma Caki cells showed that HS-1793 reduced the viability to a similar extent in both the Caki/vector and Caki/Bcl-2 cells (data not shown).

3.3. HS-1793 overcomes the resistance conferred by Bcl-2 in human leukemic U937 cells by inducing apoptosis

We next examined the mechanism by which HS-1793 overcomes the resistance conferred by Bcl-2. Since HS-1793 and resveratrol showed half-maximal inhibition of viability in U937 cells 48 h after treatment at 3 μM and 100 μM, respectively, these concentrations were used as the experimental doses. Since resveratrol at 3 μM did not show antitumor activity, 3 μM resveratrol treatment was used as an experimental control to 100 μM resveratrol treatment. In the same respect, 0.1 μM HS-1793 was used as an experimental control to 3 μM HS-1793.

Hoechst staining showed that the percentage of apoptotic cells with condensed or fragmented nuclei was not significantly reduced in 3 μM HS-1793-treated U937/Bcl-2 cell compared to 3 μM HS-1793-treated U937 cells while the percentage of these apoptotic cells was significantly reduced in 100 μM resveratrol-treated U937/Bcl-2 cells compared to the 100 μM resveratrol-treated U937 or U937/vector cells. Immunofluorescent stating to cytochrome *c* showed that translocation of cytochrome *c* from the mitochondria to the cytosol in 3 μM HS-1793-treated U937, U937/vector and U937/Bcl-2 cells and 100 μM resveratrol-treated U937 and U937/vector cells, but not in 100 μM resveratrol-treated U937/Bcl-2 cells. Mitochondrial membrane potential assay also showed that reduction of $\Delta\Psi_m$ in 3 μM HS-1793-treated U937, U937/vector and U937/Bcl-2 cells and 100 μM resveratrol-treated U937 and U937/vector cells, but not in 100 μM resveratrol-treated U937/Bcl-2 cells (Fig. 3A). DNA electrophoresis demonstrated DNA ladder in 3 μM HS-1793-treated U937/vector and U937/Bcl-2 cells and 100 μM resveratrol-treated U937/vector cells but not in 100 μM resveratrol-treated U937/Bcl-2 cells (Fig. 3B). Western blot assay showed the degradation of casapse-3 and -6 and PARP in 3 μM HS-1793-treated U937/vector and U937/Bcl-2 cells and 100 μM resveratrol-treated U937/vector cells, but not in 100 μM resveratrol-treated U937/Bcl-2 cells (Fig. 3C). Flow cytometry also demonstrated that apoptotic population was increased in 3 μM HS-1793-treated U937/vector and U937/Bcl-2 cells, and 100 μM resveratrol-treated U937/vector cells but not in 100 μM resveratrol-treated U937/Bcl-2 cells (Fig. S1). These data indicate that HS-1793 overcomes the resistance conferred by Bcl-2 by inducing apoptosis.

3.4. HS-1793 overcomes the resistance conferred by Bcl-2 in human leukemic U937 cells through 14-3-3

We next examined whether HS-1793 alters the expression level of anti-apoptotic factors. Western blot assays showed that several representative anti-apoptotic proteins such as Mcl-1, Bcl-2, Bcl-xL, XIAP, phosphorylated Akt and 14-3-3 were downregulated in cells undergoing apoptosis in response to HS-1793 or resveratrol treatment (Fig. 4A). Most previous reports showed that the expression level of the 14-3-3 protein was constantly sustained, although cells undergo apoptosis through the 14-3-3/Bad pathway. Thus, it is noticeable that HS-1793 (3 μM) and resveratrol (100 μM) markedly downregulated 14-3-3 protein to ~20% of to the controls. Importantly, whereas HS-1793 (3 μM) reduced 14-3-3 protein expression in U937/Bcl-2 cells to ~20% of the controls, resveratrol (100 μM) had no significant effect on 14-3-3 protein expression in U937/Bcl-2 cells. Since downregulation of 14-3-3 protein is bound to result in decreasing the opportunity of the association between Bad and 14-3-3, this downregualtion of 14-3-3 and subsequent modulation of the 14-3-3/Bad pathway can be speculated to be involved in overcoming the resistance conferred by Bcl-2. Thus, our further investigation was focused on 14-3-3.

Western blot assays using antibodies to two representative anti-apoptotic 14-3-3 isoforms, β and θ, demonstrated that the expression levels of both proteins were substantially downregulated in U937/vector cells in response to HS-1793 or resveratrol treatment. HS-1793, but not resveratrol, showed the corresponding downreguation in U937/Bcl-2 cells (Fig. 4B). Time-sequenced western blot assays showed that downregulation of 14-3-3 protein in cells undergoing apoptosis is evident at early time points after HS-1793 or resveratrol treatment (Fig. 4C). Conversely, the reduction of cell viability begins at later time points (Fig. 4D). These data indicate that the downregulation of 14-3-3 precedes the reduction of cell viability

We next examined whether HS-1793 exerts its antitumor activity via Bad, a representative client protein of 14-3-3. Neither HS-1793 (3 μM) nor resveratrol (100 μM) altered the expression level of total Bad protein both in U937/Vector and U937/Bcl-2 cells. Notably, downregulation of phosphor-Bad (Ser136 and 155) was observed in U937/vector cell apoptosis in response to HS-1793 (3 μM) or resveratrol (100 μM) treatment. HS-1793 (3 μM), but not resveratrol (100 μM), showed the corresponding downreguation in U937/Bcl-2 cells (Fig. 5A). Co-immunoprecipitation assays showed that the interaction between 14-3-3 and Bad is reduced in U937/vector cells in response to HS-1793 (3 μM) or resveratrol (100 μM) treatment. HS-1793 (3 μM), but not resveratrol (100 μM), showed the corresponding reduction of the interaction in U937/Bcl-2 cells (Fig. 5B). Time-sequenced western blot assays showed that the downregulation of phosphor-Bad and Bcl-2, like 14-3-3, precedes the reduction of viability (Fig. 5C). Taken together, the downregulation of 14-3-3 and subsequent modulation of the14-3-3/Bad pathway presumably plays a pivotal role in resveratrol- or HS-1793-induced apoptosis in U937 cells.

3.5. HS-1793 downregulates 14-3-3 at a post-transcriptional level in U937/Bcl-2 cells

To this end, we examined whether downreguation of 14-3-3 protein by resveratrol or HS-1793 is regulated at a transcriptional level. Our real-time PCR data indicate that the gene expression level of 14-3-3β and θ in cells undergoing apoptosis in response to HS-1793 or resveratrol treatment did not show significant differences compared to the controls (Fig. 6A). To corroborate that the downreguation of 14-3-3 protein by resveratrol or HS-1793 is not regulated at a transcriptional level, we next examined whether resveratrol and HS-1973 can affect the transcriptional level of the 14-3-3 gene family by an epigenomic regulation. Since we found the CpG islands in the 1 kb upstream regions of the 14-3-3 gene family using Methyl Primer Express® Software, and 14-3-3β is a relatively well-known isoform to exert an anti-apoptotic function, we conducted the DNA methylation and RT-PCR assay for the 14-3-3β gene. Our data show that the methylation level of the promoter regions of 14-3-3β was not changed by either resveratrol or HS-1973, indicating that the transcription of the 14-3-3β gene is not affected by methylation (Fig. 6B). We further undertook RT-PCR to examine the level of transcription of 14-3-3β. In contrast to 14-3-3β protein expression, the corresponding analysis of 14-3-3β gene expression did not demonstrate a significant difference in the relative levels of 14-3-3β mRNA in cells undergoing apoptosis in response to HS-1793 or resveratrol treatment compared to the control (Fig. 6C). Overall, these data suggest that HS-1793 or resveratrol plays a role in the downregulation of 14-3-3 at a post-transcriptional level. Furthermore, our data suggest that HS-1793 overcomes the resistance conferred by Bcl-2 in human leukemic U937 cells through downregulating 14-3-3 at a post-transcriptional level.

4. Discussion

Although resveratrol is unstable and its stilbene double bonds are readily oxidized, the simplicity of resveratrol, associated with its interesting anticancer activity, offers promise for the rational design of new chemotherapeutic agents. Previous studies reported several resveratrol analogues showing stronger antitumor effects than resveratrol. *cis*-3,5-Dimethoxy analogues of rhapontigenin and its 3′-amino and 3′-hydroxy analogues showed apoptotic activity at nanomolar concentrations [24–26]. 3′-Hydroxy stilbenes showed interesting antileukemic properties, indicating that they may constitute effective and powerful drugs in MDR and apoptosis-resistant hematological malignancies [25]. 3,4,5,4′-tetramethoxystilbene, a methoxylated derivative of resveratrol, also potently inhibited the growth of cancer cell lines [27]. 3,4′,5-Trimethoxystilbene was demonstrated to be active as an apoptotic agent at 0.24 μM [26]. In addition, it was delineated that the introduction of a naphthalene ring on the intact resveratrol molecule confers an improved ceramide-mediated proapoptotic activity [23].

Previous studies showed that the high potency of stillben analogues may be due to their preferential interaction with their receptor. In addition, the chemical configuration of the stilbene analogues may determine the subcellular sites exerting the potent apoptosis-inducing activity. It was also delineated that the potent activity of resveratrol analogues may result from their efficacy modulating the activity of several genes or kinases [28,29]. Although HS-1793 was not directly derived from resveratrol but from HS-1784, we used the term resveratrol derivative/analogue for HS-1793 since HS-1784 was derived from resveratrol. HS-1793 does not contain the unstable double bond which resveratrol has. In addition, the position of two of three hydroxyl groups in HS-1793 at the aromatic ring is different from resveratrol. Thus, we assume that these configurations of HS-1793 might confer an improved apoptosis inducing activity. To understand the mechanism by which HS-1793 exerts potent antitumor activity, further future studies are required.

14-3-3 is a family of ubiquitously expressed, dimeric proteins, consisting of seven known mammalian isoforms [30]. 14-3-3 proteins are multifunctional phosphoserine binding molecules, and one of their prominent features is the ability to bind a plethora of client proteins. Through binding with client proteins, a variety of effects can be exerted specific to the client protein. By mediating these effects in a diverse array of clients, 14-3-3 controls the cell cycle progression, mitogenic signal transduction, metabolism, oncogenesis and apoptosis. Importantly, 14-3-3 plays a critical role in cellular survival by the interaction of numerous proteins such as Bad [31]. Bad is a representative 14-3-3 client protein. Apoptotic stimuli separate Bad from 14-3-3. Bad isolated from 14-3-3 heterodimerizes with Bcl-2 and Bcl-xL, liberating Bax from those proteins to induce apoptosis [32]. The interaction of Bad with 14-3-3 is regulated extensively by phosphorylation on serine. At least three sites on Bad can be phosphorylated *in vivo*, including Ser112, Ser136, and Ser155 [31,33–35]. It is generally accepted that phosphorylation of Ser155 disrupts the interaction of Bad with Bcl-xL, which causes the translocation of Bad from the mitochondria to the cytosol, resulting in the binding of Bad to 14-3-3 [33], and phosphorylation of Ser112 and Ser136 causes the binding of Bad to 14-3-3 [31]. However, it is still controversial whether phosphorylation of Ser112 is indispensible for 14-3-3 [36].

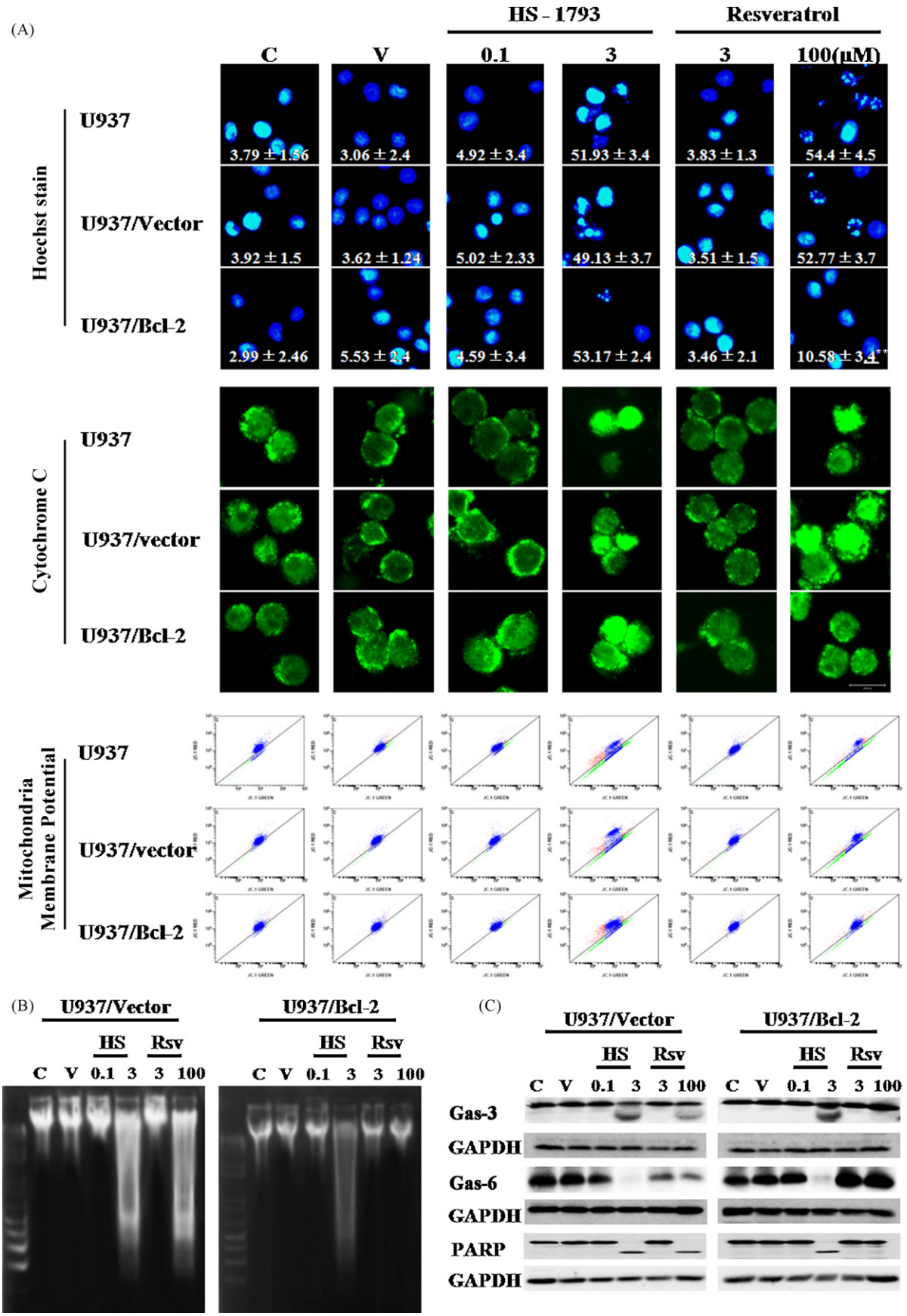

Fig. 3. HS-1793 efficiently induces apoptosis in U937/Bcl-2 cells. M, molecular marker; C, control; V, vehicle; HS, HS-1793; RSV, resveratrol. Hoechst staining showing nuclear morphology of U937 cells 48 h after resveratrol or HS-1793 treatment. Values are the mean ± S.D. percentage of apoptotic cells with condensed or fragmented nuclei. While the percentage of apoptotic cells with condensed or fragmented nuclei in 100 μM resveratrol-treated U937/Bcl-2 cells was significantly reduced compared to the 100 μM resveratrol-

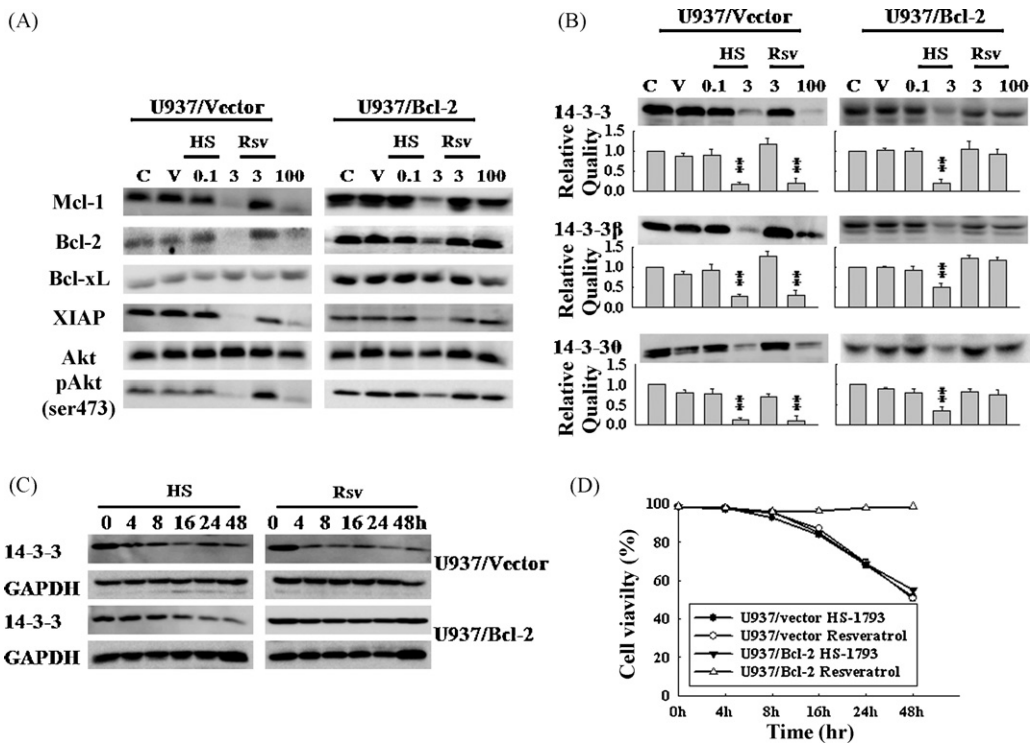

Fig. 4. HS-1793 overcomes the resistance conferred by Bcl-2 in human leukemic U937 cells through 14-3-3. Western blot assay showing downregulation of representative anti-apoptotic factors in cells undergoing apoptosis in response to resveratrol or HS-1793 treatment. Twenty-four hours after treatment (Panel A). Western blot assay showing the downreguation of 14-3-3 and 14-3-3 isoforms β and θ proteins in 3 μM HS-1793-treated U937/vector and U937/Bcl-2 cells, and 100 μM resveratrol-treated U937/vector cells but not in 100 μM resveratrol-treated U937/Bcl-2 cells. The relative intensity of the protein bands to the control is shown below each western blot data, which indicates that 14-3-3 and 14-3-3 isoforms β and θ proteins are significantly downregluated in 3 μM HS-1793-treated U937/vector and U937/Bcl-2 cells, and 100 μM resveratrol-treated U937/vector cells but not in 100 μM resveratrol-treated U937/Bcl-2 cells. $^{**}P < 0.01$ comparing to controls (U937 control and U937/vector cells). Twenty-four hours after treatment (Panel B). Time-sequenced Western blot assay showing that downregulation of 14-3-3 protein in cells undergoing apoptosis is evident at early time points after HS-1793 or resveratrol treatment. GAPDH is shown as a loading control (Panel C). Time-sequenced viability assay showing that the reduction of viability begins at later time points after HS-1793 or resveratrol treatment. See Fig. 3 for other definitions (Panel D).

Through previous studies, targeting 14-3-3 proved to provide an effective strategy to sensitize tumor cells for therapy-induced cell death. Reduction of 14-3-3 levels increased the sensitivity of lung adenocarcinoma cells to ionizing radiation [37], and 14-3-3 deletion was correlated with the increased sensitivity of colorectal cancer cells to doxorubicin-induced apoptosis [38]. Furthermore, deletion of 14-3-3 in yeast resulted in hypersensitivity to rapamycin, an mTOR inhibitor [39,40], and knockdown of 14-3-3 in MCF7/AdrVp3000 by siRNA increased the sensitivity of these cells to doxorubicin. 14-3-3 was also found upregulated in a drug-resistant pancreatic adenocarcinoma cell line [41,42]. These observations strongly enhance the rationale for the development of specific 14-3-3 inhibitors as anticancer agents, both alone and in combination with other targeted agents.

Most chemotherapeutic agents have been delineated not to alter the expression level of 14-3-3 protein, although they exert antitumor activity via the 14-3-3/Bad pathway. Only a few chemotherapeutic agents have been documented to down-regulate 14-3-3 in cells undergoing apoptosis via the 14-3-3/Bad pathway [43–46]. In the present study, we first revealed that the antitumor activity of HS-1793, as well as resveratrol, is mediated by the downregulation of 14-3-3 which seems, at least in part, to play a role in resveratrol- or HS-1793-induced apoptosis in U937 cells.

Our data suggest that HS-1793 could be a novel therapeutic strategy for overcoming the resistance conferred by Bcl-2. However, it remains an open question through which exact mechanism(s) HS-1793 downregulates 14-3-3 in Bcl-2 over-expressing U937 cells. At this moment, only a few studies in the literature provide fragmentary information on this question. In a previous study, we demonstrated that the sustained activation of Akt by the overexpression of Bcl-2 is involved in the attenuation of chemotherapeutic-induced apoptosis [44]. In the present study, we also observed the sustained activation of Akt in resveratrol-treated Bcl-2 overexpressing U937 cells. Although these data suggest that Bcl-2 may be involved in the stabilization of 14-3-3 via Akt, a detailed molecular mechanism remains to be delineated. It also remains to be determined exactly how 14-3-3

treated U937 or U937/vector cells, the percentage of apoptotic cells with condensed or fragmented nuclei showing the nuclear condensation or fragmentation in 3 μM HS-1793-treated U937/Bcl-2 cells was not significantly reduced. $^{**}P < 0.01$. Immunofluorescent stating to cytochrome *c* shows that translocation of cytochrome *c* from the mitochondria to the cytosol in 3 μM HS-1793-treated U937, U937/vector and U937/Bcl-2 cells and 100 μM resveratrol-treated U937 and U937/vector cells, but not in 100 μM resveratrol-treated U937/Bcl-2 cells. Mitochondrial membrane potential assay shows that reduction of $\Delta\Psi_m$ is observed in 3 μM HS-1793-treated U937, U937/vector and U937/Bcl-2 cells and 100 μM resveratrol-treated U937 and U937/vector cells, but not in 100 μM resveratrol-treated U937/Bcl-2 cells. Bar, 20 μm (Panel A). DNA electrophoresis conducted on the cells harvested 48 h after treatment. DNA ladder was demonstrated in 3 μM HS-1793-treated U937/vector and U937/Bcl-2 cells and 100 μM resveratrol-treated U937/vector cells but not in 100 μM resveratrol-treated U937/Bcl-2 cells (Panel B). Western blot assay showing activation of caspase-3 and -6. Degradation of casapse-3 and -6 and PARP are shown in 3 μM HS-1793-treated U937/vector and U937/Bcl-2 cells and 100 μM resveratrol-treated U937/vector cells, but not in 100 μM resveratrol-treated U937/Bcl-2 cells. GAPDH is shown as a loading control (Panel C).

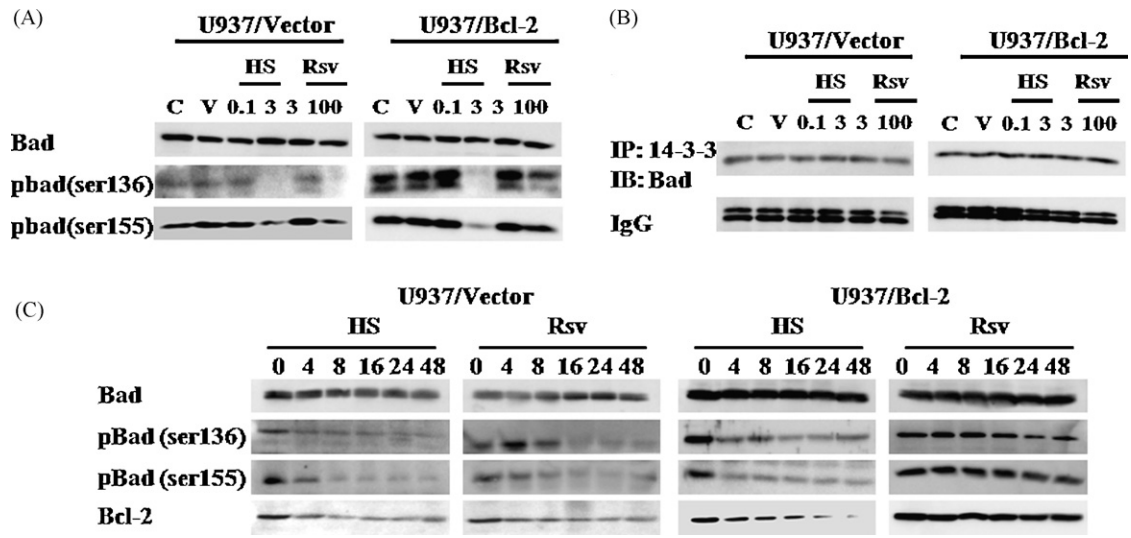

Fig. 5. HS-1793 exerts its antitumor activity via Bad. Western blot assay showing total Bad and phosphor Bad (Ser136 and 155) proteins expression level. 48 h after treatment (Panel A). Co-immunoprecipitation assay showing the interaction between 14-3-3 and Bad. IgG is shown as a loading control (Panel B). Time-sequenced Western blot assay showing the alteration of Bad, phosphor Bad (Ser136 and 155) and Bcl-2 expression level after HS-1793 or resveratrol treatment. See Fig. 3 for other definitions (Panel C).

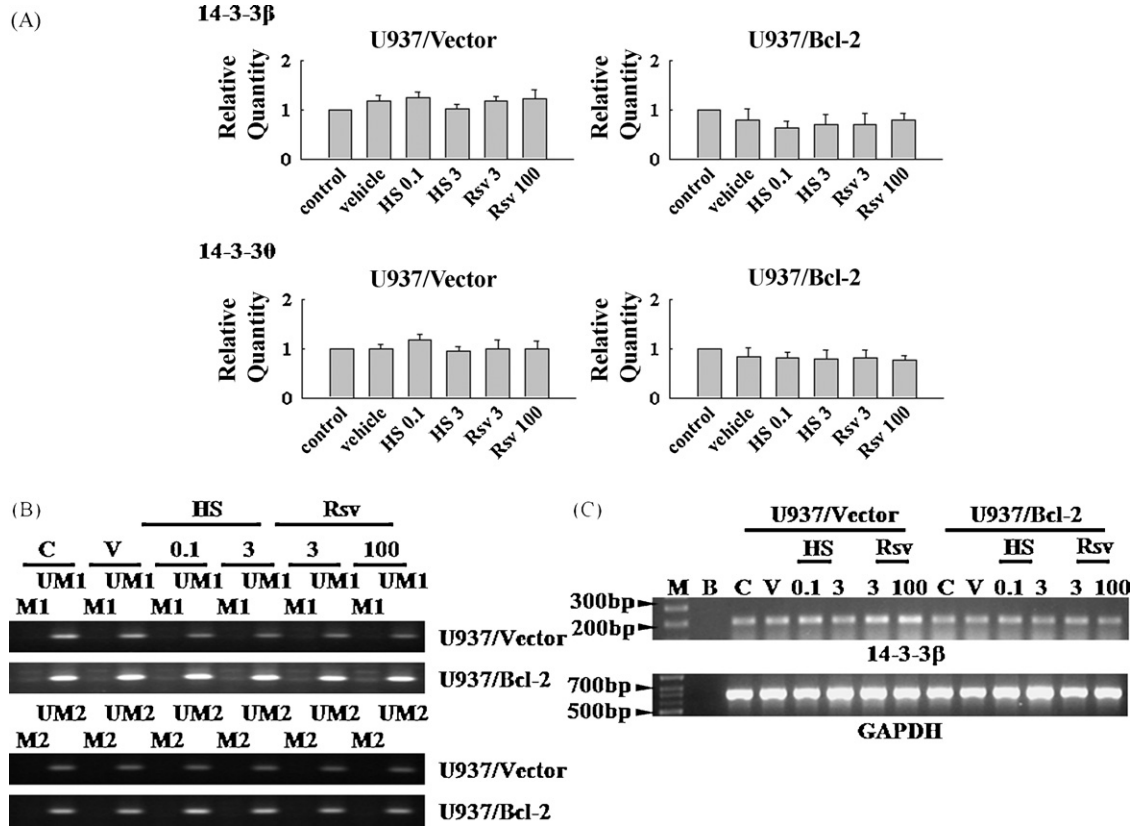

Fig. 6. HS-1793 plays a role in the downregulation of 14-3-3 at a post-transcriptional level. Real-time PCR data showing the gene expression level of 14-3-3β and θ in cells undergoing apoptosis in response to HS-1793 or resveratrol treatment (Panel A). A representative DNA methylation specific PCR analysis 14-3-3β gene. UM, reaction with primers specific for the unmethylated target. M: reaction with primers specific for the methylated target. Primer sets used for amplification are designated M1, UM1, M2 and UM2 (Panel B). A representative RT-PCR assay for the 14-3-3β gene. The levels of GAPDH served as loading controls. B, Blank. See Fig. 3 for other definitions (Panel C).

is regulated post-transcriptionally in Bcl-2 overexpressing U937 cells by HS-1793, but not resveratrol. The answer to these questions may guide the development of novel anticancer drugs targeting 14-3-3 to overcome the resistance conferred by Bcl-2.

In summary, a novel resveratrol derivative, HS-1793, overcomes the resistance conferred by Bcl-2 in human leukemic U937 cells via 14-3-3.

Conflicts of interest

No potential conflicts of interest were disclosed.

Acknowledgement

Supported from a grant: Korea Research Foundation Grant KRF-2006-J03501.

Appendix A. Supplementary data

Supplementary data associated with this article can be found, in the online version, at doi:10.1016/j.bcp.2009.01.002.

References

[1] Tsujimoto Y, Croce CM. Analysis of the structure, transcripts and protein products of bcl-2, the gene involved in human follicular lymphoma. Proc Natl Acad Sci USA 1986;83:5214–8.
[2] Kluck RM, Bossy-Wetzel E, Green DR, Newmeyer DD. The release of cytochrome *c* from mitochondria: a primary site for Bcl-2 regulation of apoptosis. Science 1997;275:1132–6.
[3] Dasmahapatra G, Almenara JA, Grant S. Flavopiridol and histone deacetylase inhibitors promote mitochondrial injury and cell death in human leukemia cells that overexpress Bcl-2. Mol Pharmacol 2006;69:288–98.
[4] Yin XM, Oltvai ZN, Korsmeyer SJ. BH1 and BH2 domains of Bcl-2 are required for inhibition of apoptosis and heterodimerization with Bax. Nature 1994;369:321–3.
[5] Yin DX, Schimke RT. BCL-2 expression delays drug-induced apoptosis but does not increase clonogenic survival after drug treatment in HeLa cells. Cancer Res 1995;55:4922–8.
[6] Park JW, Choi YJ, Suh SI, Baek WK, Suh MH, Jin IN, et al. Bcl-2 overexpression attenuates resveratrol-induced apoptosis in U937 cells by inhibition of caspase-3 activity. Carcinogenesis 2001;22:1633–9.
[7] Campos L, Rouault JP, Sabido O, Oriol P, Roubi N, Vasselon C, et al. High expression of bcl-2 protein in acute myeloid leukemia cells is associated with poor response to chemotherapy. Blood 1993;81:3091–6.
[8] Lowenberg B, Downing JR, Burnett A. Acute myeloid leukemia. N Engl J Med 1999;341:1051–62.
[9] Smith M, Barnett M, Bassan R, Gatta G, Tondini C, Kern W. Adult acute myeloid leukaemia. Crit Rev Oncol Hematol 2004;50:197–222.
[10] Gusman J, Malonne H, Atassi G. A reappraisal of the potential chemopreventive and chemotherapeutic properties of resveratrol. Carcinogenesis 2001;22:1111–7.
[11] Frémont L. Biological effects of resveratrol. Life Sci 2000;66:663–73.
[12] Kotha A, Sekharam M, Cilenti L, Siddiquee K, Khaled A, Zervos AS, et al. Resveratrol inhibits Src and Stat3 signaling and induces the apoptosis of malignant cells containing activated Stat3 protein. Mol Cancer Ther 2006;5:621–9.
[13] Woo KJ, Lee TJ, Lee SH, Lee JM, Seo JH, Jeong YJ, et al. Elevated gadd153/chop expression during resveratrol-induced apoptosis in human colon cancer cells. Biochem Pharmacol 2007;73:68–76.
[14] Ulrich S, Wolter F, Stein JM. Molecular mechanisms of the chemopreventive effects of resveratrol and its analogs in carcinogenesis. Mol Nutr Food Res 2005;49:452–61.
[15] Zhang W, Fei Z, Zhen HN, Zhang JN, Zhang X. Resveratrol inhibits cell growth and induces apoptosis of rat C6 glioma cells. J Neurooncol 2007;81:231–40.
[16] Cecchinato V, Chiaramonte R, Nizzardo M, Cristofaro B, Basile A, Sherbet GV, et al. Resveratrol-induced apoptosis in human T-cell acute lymphoblastic leukaemia MOLT-4 cells. Biochem Pharmacol 2007;74:1568–74.
[17] Clément MV, Hirpara JL, Chawdhury SH, Pervaiz S. Chemopreventive agent resveratrol, a natural product derived from grapes, triggers CD95 signaling-dependent apoptosis in human tumor cells. Blood 1998;92:996–1002.
[18] Lee EO, Kwon BM, Song GY, Chae CH, Kim HM, Shim IS, et al. Heyneanol A induces apoptosis via cytochrome *c* release and caspase activation in human leukemic U937 cells. Life Sci 2004;74:2313–26.
[19] Song S, Lee H, Jin Y, Ha YM, Bae S, Chung HY, et al. Syntheses of hydroxy substituted 2-phenyl-naphthalenes as inhibitors of tyrosinase. Bioorg Med Chem Lett 2007;17:461–4.
[20] Rho JH, Kang DY, Park KJ, Choi HJ, Lee HS, Yee SB, et al. Doxorubicin induces apoptosis with profile of large-scale DNA fragmentation and without DNA ladder in anaplastic thyroid carcinoma cells via histone hyperacetylation. Int J Oncol 2005;27:465–71.
[21] Park SE, Kim ND, Yoo YH. Acetylcholinesterase plays a pivotal role in apoptosome formation. Cancer Res 2004;64:2652–5.
[22] Mewshaw RE, Edsall Jr RJ, Yang C, Manas ES, Xu ZB, Henderson RA, et al. ERbeta ligands. 3. Exploiting two binding orientations of the 2-phenylnaphthalene scaffold to achieve ERbeta selectivity. J Med Chem 2005;48:3953–79.
[23] Minutolo F, Sala G, Bagnacani A, Bertini S, Carboni I, Placanica G, et al. Synthesis of a resveratrol analogue with high ceramide-mediated proapoptotic activity on human breast cancer cells. J Med Chem 2005;48:6783–6.
[24] Roberti M, Pizzirani D, Recanatini M, Simoni D, Grimaudo S, Di Cristina A, et al. Identification of a terphenyl derivative that blocks the cell cycle in the G0-G1 phase and induces differentiation in leukemia cells. J Med Chem 2006;49:3012–8.
[25] Tolomeo M, Grimaudo S, Di Cristina A, Roberti M, Pizzirani D, Meli M, et al. Pterostilbene and 3′-hydroxypterostilbene are effective apoptosis-inducing agents in MDR and BCR-ABL-expressing leukemia cells. Int J Biochem Cell Biol 2005;37:1709–26.
[26] Simoni D, Roberti M, Invidiata FP, Aiello E, Aiello S, Marchetti P, et al. Stilbene-based anticancer agents: resveratrol analogues active toward HL60 leukemic cells with a non-specific phase mechanism. Bioorg Med Chem Lett 2006;16:3245–8.
[27] Gosslau A, Chen M, Ho CT, Chen KY. A methoxy derivative of resveratrol derivative selectively induced activation of the mitochondrial apoptotic pathway in transformed fibroblasts. Br J Cancer 2005;92:513–21.
[28] Lee KW, Kang NJ, Rogozin EA, Oh S, Heo YS, Pugliese A, et al. The resveratrol analogue 3,5,30,40,50-pentahydroxy-trans-stilbene inhibits cell transformation via MEK. Int J Cancer 2008;123:2487–96.
[29] Gosslau A, Pabbaraja S, Knapp S, Chen KY. Trans- and cis-stilbene polyphenols induced rapid perinuclear mitochondrial clustering and p53-independent apoptosis in cancer cells but not normal cells. Eur J Pharm 2008;587:25–34.
[30] Fu H, Subramanian RR, Masters SC. 14-3-3 Proteins: structure, function, and regulation. Annu Rev Pharmacol Toxicol 2000;40:617–47.
[31] Zha J, Harada H, Yang E, Jockel J, Korsmeyer SJ. Serine phosphorylation of death agonist BAD in response to survival factor results in binding to 14-3-3 not BCL-X(L). Cell 1996;87:619–28.
[32] Yang E, Zha J, Jockel J, Boise LH, Thompson CB, Korsmeyer SJ. Bad, a heterodimeric partner for Bcl-XL and Bcl-2, displaces Bax and promotes cell death. Cell 1995;80:285–91.
[33] Datta SR, Katsov A, Hu L, Petros A, Fesik SW, Yaffe MB, et al. 14-3-3 proteins and survival kinases cooperate to inactivate BAD by BH3 domain phosphorylation. Mol Cell 2000;6:41–51.
[34] Lizcano JM, Morrice N, Cohen P. Regulation of BAD by cAMP-dependent protein kinase is mediated via phosphorylation of a novel site, Ser155. Biochem J 2000;349:547–57.
[35] Zhou XM, Liu Y, Payne G, Lutz RJ, Chittenden T. Growth factors inactivate the cell death promoter BAD by phosphorylation of its BH3 domain on Ser155. J Biol Chem 2000;275:25046–51.
[36] Masters SC, Yang H, Datta SR, Greenberg ME, Fu H. 14-3-3 inhibits Bad-induced cell death through interaction with serine-136. Mol Pharmacol 2001;60:1325–31.
[37] Qi W, Martinez JD. Reduction of 14-3-3 proteins correlates with increased sensitivity to killing of human lung cancer cells by ionizing radiation. Radiat Res 2003;160:217–23.
[38] Chan TA, Hwang PM, Hermeking H, Kinzler KW, Vogelstein B. Cooperative effects of genes controlling the G(2)/M checkpoint. Genes Dev 2000;14:1584–8.
[39] Bertram PG, Zeng C, Thorson J, Shaw AS, Zheng XF. The 14-3-3 proteins positively regulate rapamycin-sensitive signalling. Curr Biol 1998;8:1259–67.
[40] Bjornsti MA, Houghton PJ. The TOR pathway: a target for cancer therapy. Nat Rev Cancer 2004;4:335–48.
[41] Liu Y, Liu H, Han B, Zhang JT. Identification of 14-3-3sigma as a contributor to drug resistance in human breast cancer cells using functional proteomic analysis. Cancer Res 2006;66:3248–55.
[42] Sinha P, Hütter G, Köttgen E, Dietel M, Schadendorf D, Lage H. Increased expression of epidermal fatty acid binding protein, cofilin, and 14-3-3-sigma (stratifin) detected by two-dimensional gel electrophoresis, mass spectrometry and microsequencing of drug-resistant human adenocarcinoma of the pancreas. Electrophoresis 1999;20:2952–60.
[43] Tudor G, Aguilera A, Halverson DO, Laing ND, Sausville EA. Susceptibility to drug-induced apoptosis correlates with differential modulation of Bad, Bcl-2 and Bcl-xL protein levels. Cell Death Differ 2000;7:574–86.
[44] Ngan CY, Yamamoto H, Takagi A, Fujie Y, Takemasa I, Ikeda M, et al. Oxaliplatin induces mitotic catastrophe and apoptosis in esophageal cancer cells. Cancer Sci 2008;99:129–39.
[45] Yee SB, Baek SJ, Park HT, Jeong SH, Jeong JH, Kim TH, et al. zVAD-fmk, unlike BocD-fmk, does not inhibit caspase-6 acting on 14-3-3/Bad pathway in apoptosis of p815 mastocytoma cells. Exp Mol Med 2006;38:634–42.
[46] Woo KJ, Yoo YH, Park JW, Kwon TK. Bcl-2 attenuates anticancer agents-induced apoptosis by sustained activation of Akt/protein kinase B in U937 cells. Apoptosis 2005;10:1333–43.